Timing Jitter

Variations of the pulse positions or sampling instants cause timing jitter. This results from several causes, some of which are dependent on the pulse pattern being transmitted, whereas others are not. The former are cumulative along the chain of regenerative repeaters, since all the repeaters are affected in the same way, whereas the other forms of jitter are random from regenerator to regenerator and therefore tend to partially cancel out their mutual effects over a long-haul link. Random forms of jitter are caused by noise, interference, and mistuning of the clock circuits. Pattern-dependent jitter results from clock mistuning, amplitude-to-phase conversion in the clock circuit, and ISI, which alters the position of the peaks of the input signal according to the pattern. The rms value of the jitter over a long chain of N repeaters can be shown to increase as $\sqrt{N}$.

Jitter accumulation over a digital link may be reduced by buffering the link with an elastic store and clocking out the digit stream under the control of a highly stable phase-locked loop. Jitter reduction is necessary about every 200 miles in a long digital link to keep the maximum jitter within reasonable limits.

7.5.3 Detection Error

Once the transmission has passed through the equalizer, detection can take place at the detector that samples the received signal based on the clock provided by the timing extractor. The signal received at the detector consists of the equalized pulse train plus a random channel noise. The noise can cause error in pulse detection. Consider, for example, the case of polar transmission using a basic pulse $p(t)$ (Fig. 7.24a). This pulse has a peak amplitude A_p. A typical received pulse train is shown in Fig. 7.24b. Pulses are sampled at their peak values. If noise were absent, the sample of the positive pulse (corresponding to **1**) would be A_p and that of the negative pulse (corresponding to **0**) would be $-A_p$.* Because of noise, these samples would be $\pm A_p + n$ where n is the random noise amplitude (see Fig. 7.24b). From the symmetry of the situation, the detection threshold is zero; that is, if the pulse sample value is positive, the digit is detected as **1**; if the sample value is negative, the digit is detected as **0**.

Figure 7.24 Error probability in threshold detection.

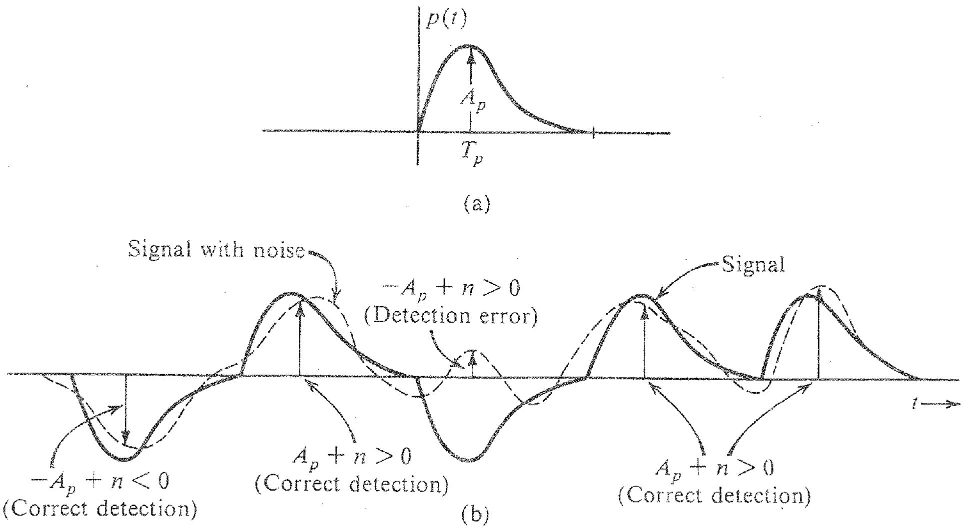

* This assumes zero ISI.

The detector's decision of whether to declare **1** or **0** could be made readily from the pulse sample, except that the noise value n is random, meaning that its exact value is unpredictable. It may have a large or a small value, and it can be negative as well as positive. It is possible that **1** is transmitted but n at the sampling instant has a large negative value. This will make the sample value $A_p + n$ small or even negative. On the other hand, if **0** is transmitted and n has a large positive value at the sampling instant, the sample value $-A_p + n$ can be positive and the digit will be detected wrongly as **1**. This is clear from Fig. 7.24b.

The performance of digital communication systems is typically specified by the average number of detection errors. For example, if two cellphones (receivers) in the same spot are attempting to detect the same transmission from a cellular tower, the cellphone with the lower number of detection errors is the better receiver. It is likely to have fewer dropped calls and less trouble receiving clear speech. However, because noise is random, sometimes one cellphone may be better while other times the other cellphone may have fewer errors. The real measure of receiver performance is therefore the average ratio of the number of errors to the total number of transmitted data. Thus, the meaningful performance comparison is the likelihood of detection error, or the **detection error probability**.

Because the precise analysis and evaluation of this error likelihood require the knowledge and tools from probability theory, we will postpone error analysis until after the introduction of probability in Chapter 8. Later, in Chapter 10, we will discuss fully the error probability analysis of different digital communication systems for different noise models as well as system designs against different noises. For example, Gaussian noise can generally characterize the random channel noise from thermal effects and intersystem cross talk. Optimum detectors can be designed to minimize the error likelihood against Gaussian noise. However, switching transients, lightning strikes, power line load switching, and other singular events cause very high level noise pulses of short duration to contaminate the cable pairs that carry digital signals. These pulses, collectively called **impulse noise**, cannot conveniently be engineered away, and they constitute the most prevalent source of errors from the environment outside the digital systems. Errors are virtually never, therefore, found in isolation, but occur in bursts of up to several hundred at a time. To correct error burst, we use special **burst error correcting codes** described in Chapter 14.

7.6 EYE DIAGRAMS: AN IMPORTANT TOOL

In the last section, we studied the effect of noise and channel ISI on the detection of digital transmissions. We also described the design of equalizers to compensate the channel distortion and explained the timing-extraction process. We now present a practical engineering tool known as the **eye diagram**. The eye diagram is easy to generate and is often applied by engineers on received signals because it makes possible the visual examination of severity of the ISI, the accuracy of timing extraction, the noise immunity, and other important factors.

We need only a basic oscilloscope to generate the eye diagram. Given a baseband signal at the channel output

$$y(t) = \sum a_k p(t - kT_b)$$

it can be applied to the vertical input of the oscilloscope. The time base of the scope is triggered at the same rate $1/T_b$ as that of the incoming pulses, and it yields a sweep lasting exactly T_b, the interval of one transmitted data symbol a_k. The oscilloscope shows the superposition of

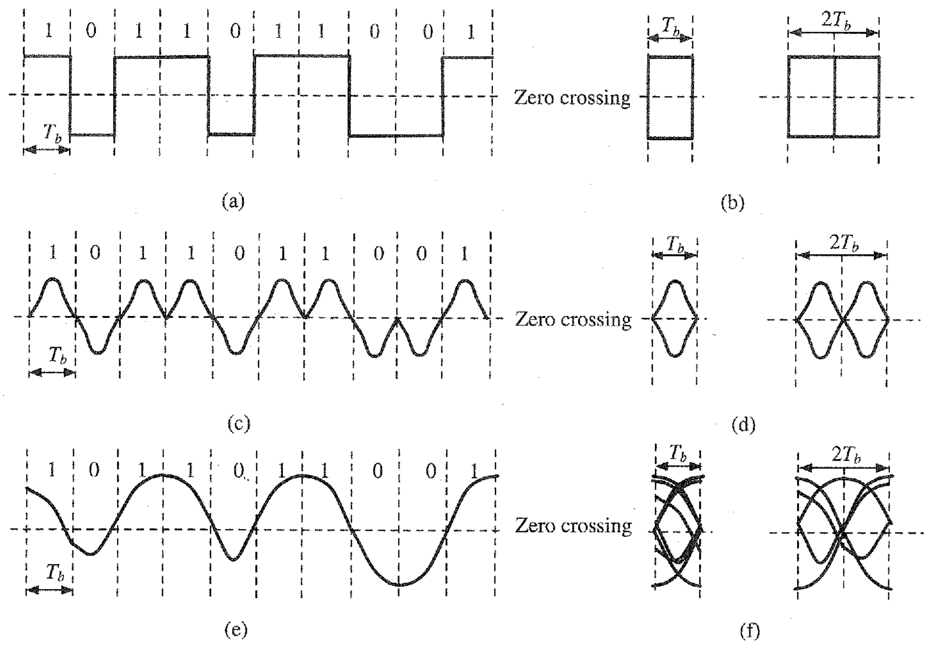

Figure 7.25 The eye diagram.

many traces of length T_b from the channel output $y(t)$. What appears on the oscilloscope is simply the input signal (vertical input) cut up every T_b and then superimposed on top of one another. The resulting pattern on the oscilloscope looks like a human eye, hence the name eye diagram. More generally, we can also apply a time sweep that lasts m symbol intervals, or mT_b. The oscilloscope pattern is simply the input signal (vertical input) cut up every mT_b and then superimposed on top of one another. The oscilloscope will then display an eye diagram that is mT_b wide and has the shape of m eyes in a horizontal row.

We now present an example. Consider the transmission of a binary signal by polar NRZ pulses (Fig. 7.25a). Its eye diagrams are shown in Fig. 7.25b for the time base of T_b and $2T_b$, respectively. In this example, the channel has infinite bandwidth to pass the NRZ pulse and there is no channel distortion. Hence, we obtain eye diagrams with totally *open* eye(s). We can also consider a channel output using the same polar line code and a different (RZ) pulse shape, as shown in Fig. 7.25c. The resulting eye diagrams are shown in Fig. 7.25d. In this case, the eye is wide open only at the midpoint of the pulse duration. With proper timing extraction, the receiver should sample the received signal right at the midpoint where the eye is totally open, to achieve the best noise immunity at the decision point (Sec. 7.5.3). This is because the midpoint of the eye represents the best sampling instant of each pulse, where the pulse amplitude is maximum without interference from any other neighboring pulse (zero ISI).

We now consider a channel that is distortive or has finite bandwidth, or both. After passing through this nonideal channel, the NRZ polar signal of Fig. 7.25a becomes the waveform of Fig. 7.25e. The received signal pulses are no longer rectangular but are be rounded, distorted, and spread out. The eye diagrams are not fully open anymore, as shown in Fig. 7.25f. In this case, the ISI is not zero. Hence, pulse values at their respective sampling instants will deviate from the full-scale values by a varying amount in each trace, causing blurs, resulting in a partially closed eye pattern.

In the presence of channel noise, the eye will tend to close in all cases. Weaker noise will cause proportionately less closing. The decision threshold with respect to which symbol

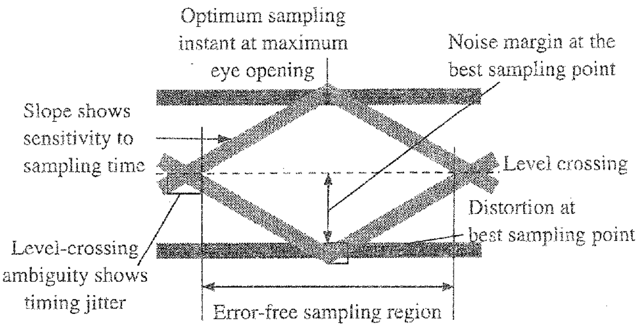

Figure 7.26 Reading an eye diagram.

(1 or 0) was transmitted is the midpoint of the eye.* Observe that for zero ISI, the system can tolerate noise of up to half the vertical opening of the eye. Any noise value larger than this amount can cause a decision error if its sign is opposite to the sign of the data symbol. Because ISI reduces the eye opening, it clearly reduces noise tolerance. The eye diagram is also used to determine optimum tap settings of the equalizer. Taps are adjusted to obtain the maximum vertical and horizontal eye opening.

The eye diagram is a very effective tool for signal analysis during real-time experiments. It not only is simple to generate, it also provides very rich and important information about the quality and susceptibility of the received digital signal. From the typical eye diagram given in Fig. 7.26, we can extract several key measures regarding the signal quality.

- *Maximum opening point.* The eye opening amount at the sampling and decision instant indicates that amount of noise the detector can tolerate without making an error. The quantity is known as the *noise margin*. The instant of maximum eye opening indicates the optimum sampling or decision-making instant.
- *Sensitivity to timing jitter.* The width of the eye indicates the time interval over which correct decision can still be made, and it is desirable to have an eye with the maximum horizontal opening. If the decision-making instant deviates from the instant when the eye has a maximum vertical opening, the margin of noise tolerance is reduced. This causes higher error probability in pulse detection. The slope of the eye shows how fast the noise tolerance is reduced and, hence, the sensitivity of the decision noise tolerance to variation of the sampling instant. It demonstrates the effects of timing jitter.
- *Level-crossing (timing) jitter.* Typically, practical receivers extract timing information about the pulse rate and the sampling clock from the (zero) level crossing of the received signal waveform. The variation of level crossing can be seen from the width of the eye corners. This measure provides information about the timing jitter such a receiver is expected to experience.

Finally, we provide a practical eye diagram example for a polar signaling waveform. In this case, we select a cosine roll-off pulse that satisfy Nyquist's first criterion of zero ISI. The roll-off factor is chosen to be $r = 0.5$. The eye diagram is shown in Fig. 7.27 for a time base of $2T_b$. In fact, even for the same signal, the eye diagrams may be somewhat different for different time offset (or initial point) values. Figure 7.27a illustrates the eye diagram of this polar signaling waveform for a display time offset of $T_b/2$, whereas Fig. 7.27b shows the

* This is true for a two-level decision [e.g., when $p(t)$ and $-p(t)$ are used for **1** and **0**, respectively]. For a three-level decision (e.g., bipolar signaling), there will be two thresholds.

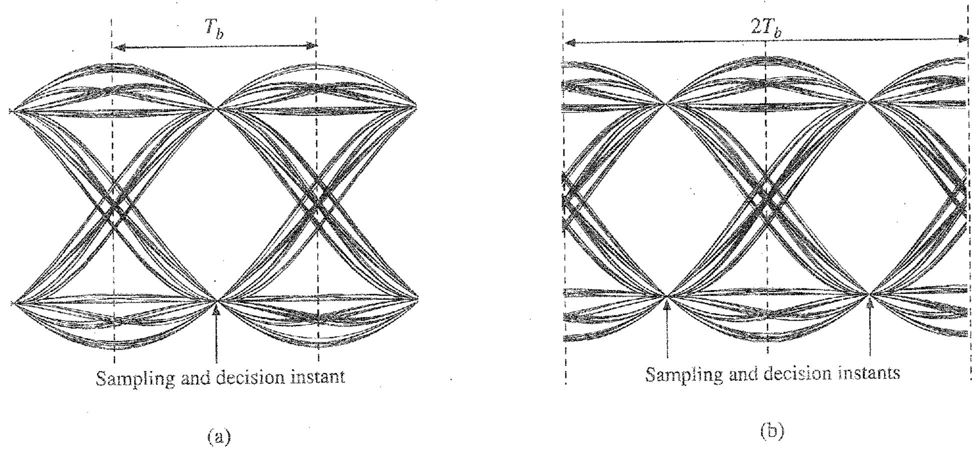

Figure 7.27 Eye diagrams of a polar signaling system using a raised cosine pulse with roll-off factor 0.5: (a) over 2 symbol periods $2T_b$ with a time shift $T_b/2$; (b) without time shift.

normal eye diagram when the display time offset value is zero. It is clear from comparison that these two diagrams have a simple horizontal circular shift relationship. By observing the maximum eye opening, we can see that this baseband signal has zero ISI, confirming the basic feature of the raised-cosine pulse. On the other hand, because Nyquist's first criterion places no requirement on the zero crossing of the pulse, the eye diagram indicates that timing jitter would be likely.

7.7 PAM: M-ARY BASEBAND SIGNALING FOR HIGHER DATA RATE

Regardless of which line code is used, binary baseband modulations have one thing in common: they all transmit one bit of information over the interval of T_b second, or at the bit rate of $1/T_b$ bit per second. If the transmitter would like to send bits at a much higher rate, T_b may be shortened. For example, to increase the bit rate by M, T_b must be reduced by the same factor of M; however, there is a heavy price to be paid in bandwidth. As we demonstrated in Fig. 7.9, the bandwidth of baseband modulation is proportional to the pulse rate $1/T_b$. Shortening T_b by a factor of M will certainly increase the required channel bandwidth by M. Fortunately, reducing T_b is not the only way to increase data rate. A very effective practical solution is to allow each pulse to carry multiple bits. We explain this concept here.

For each symbol transmission within the time interval of T_b to carry more bits, there must be more than two symbols to choose from. By increasing the number of symbols to M, we ensure that the information transmitted by each symbol will also increase with M. For example, when $M = 4$ (4-ary, or quaternary), we have four basic symbols, or pulses, available for communication (Fig. 7.28a). A sequence of two binary digits can be transmitted by just one 4-ary symbol. This is because a sequence of two bits can form only four possible sequences (viz., **11**, **10**, **01**, and **00**). Because we have four distinct symbols available, we can assign one of the four symbols to each of these combinations (Fig. 7.28a). Each symbol now occupies a time duration of T_s. A signaling example for a short sequence is given in Fig. 7.28b and the 4-ary eye-diagram is shown in Fig. 7.28c.

This signaling allows us to transmit each pair of bits by one 4-ary pulse (Fig. 7.28b). Hence, to transmit n bits, we need only $(n/2)$ 4-ary pulses. This means one 4-ary symbol can transmit the information of two binary digits. Also, because three bits can form $2 \times 2 \times 2 = 8$ combinations, a group of three bits can be transmitted by one 8-ary symbol. Similarly, a group

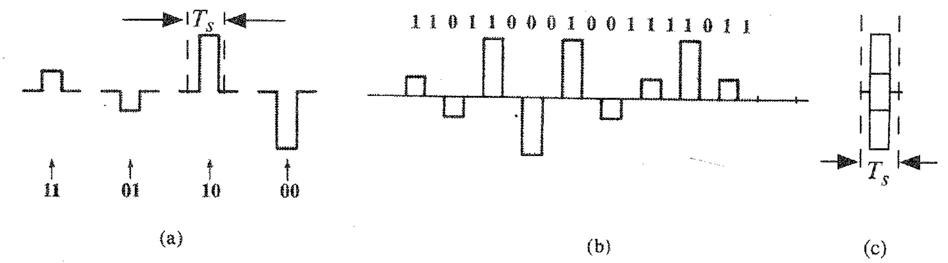

Figure 7.28 4-Ary PAM signaling: (a) four RZ symbols; (b) baseband transmission; (c) the 4-ary RZ eye diagram.

of four bits can be transmitted by one 16-ary symbol. In general, the information I_M transmitted by an M-ary symbol is

$$I_M = \log_2 M \text{ bits} \tag{7.55}$$

This means we can increase the rate of information transmission by increasing M.

This special M-ary signaling is known as the **pulse amplitude modulation (PAM)** because the data information is conveyed by the varying pulse amplitude. We should note here that pulse amplitude modulation is only one of many possible choices of M-ary signaling. There are an infinite number of such choices. Still, only a limited few are truly effective in combating noise and efficient in saving bandwidth and power. A more detailed discussion of other M-ary signaling schemes will be presented a little later, in Sec. 7.9.

As in most system designs, there are always prices to pay for every possible gain. The price paid by PAM to increase data rate is power. As M increases, the transmitted power also increases as M. This is because to have the same noise immunity, the minimum separation between pulse amplitudes should be comparable to that of binary pulses. Therefore, pulse amplitudes increase with M (Fig. 7.28). It can be shown that the transmitted power increases as M^2 (Prob. 7.7-5). Thus, to increase the rate of communication by a factor of $\log_2 M$, the power required increases as M^2. Because the transmission bandwidth depends only on the pulse rate and not on pulse amplitudes, the bandwidth is independent of M. We will use the following example of PSD analysis to illustrate this point.

Example 7.4

Determine the PSD of the quaternary (4-ary) baseband signaling in Fig. 7.28 when the message bits **1** and **0** are equally likely.

The 4-ary line code has four distinct symbols corresponding to the four different combinations of two message bits. One such mapping is

$$a_k = \begin{cases} -3 & \text{message bits 00} \\ -1 & \text{message bits 01} \\ +1 & \text{message bits 10} \\ +3 & \text{message bits 11} \end{cases} \tag{7.56}$$

Therefore, all four values of a_k are equally likely, each with a chance of 1 in 4. Recall that

$$R_0 = \lim_{N\to\infty} \frac{1}{N} \sum_k a_k^2$$

Within the summation, 1/4 of the a_k will be ± 1, and ± 3. Thus,

$$R_0 = \lim_{N\to\infty} \frac{1}{N}\left[\frac{N}{4}(-3)^2 + \frac{N}{4}(-1)^2 + +\frac{N}{4}(1)^2 + +\frac{N}{4}(3)^2\right] = 5$$

On the other hand, for $n > 0$, we need to determine

$$R_n = \lim_{N\to\infty} \frac{1}{N}\sum_k a_k a_{k+n}$$

To find this average value, we build a table with all the possible values of the product $a_k a_{k+n}$:

Possible Values of $a_k a_{k+n}$

a_{k+n} \ a_k	−3	−1	+1	+3
−3	9	3	−3	−9
−1	3	1	−1	−3
+1	−3	−1	1	3
+3	−9	−3	3	9

From the foregoing table listing all the possible products of $a_k a_{k+n}$, we see that each product in the summation $a_k a_{k+n}$ can take on any of the following six values ± 1, ± 3, ± 9. First, (± 1, ± 9) are equally likely (1 in 8). On the other hand, ± 3 are equally likely (1 in 4). Thus, we can show that

$$R_n = \lim_{N\to\infty} \frac{1}{N}\left[\frac{N}{8}(-9) + \frac{N}{8}(+9) + \frac{N}{8}(-1) + \frac{N}{8}(+1) + \frac{N}{4}(-3) + \frac{N}{4}(+3)\right] = 0$$

As a result,

$$S_x(f) = \frac{5}{T_s} \quad \Longrightarrow \quad S_y(f) = \frac{5}{T_s}\,|P(f)|^2$$

Thus, the M-ary line code generates the same PSD shape as binary polar signaling. The only difference is that it utilizes 5 times the original signal power.

Although most terrestrial digital telephone network uses binary encoding, the subscriber loop portion of the integrated services digital network (ISDN) uses the quaternary code, 2B1Q, similar to Fig. 7.28a. It uses NRZ pulses to transmits 160 kbit/s of data at a **baud** rate (pulse rate) of 80 kbit/s. Of the various line codes examined by the ANSI standards committee, 2B1Q provided the greatest baud rate reduction in the noisy and cross-talk-prone local cable plant environment.

Pulse Shaping and Eye Diagrams in PAM: In this case, we can use the Nyquist criterion pulses because these pulses have zero ISI at the sample points, and, therefore, their amplitudes can be correctly detected by sampling at the pulse centers. We can also use the controlled ISI (partial-response signaling) for M-ary signaling.[8]

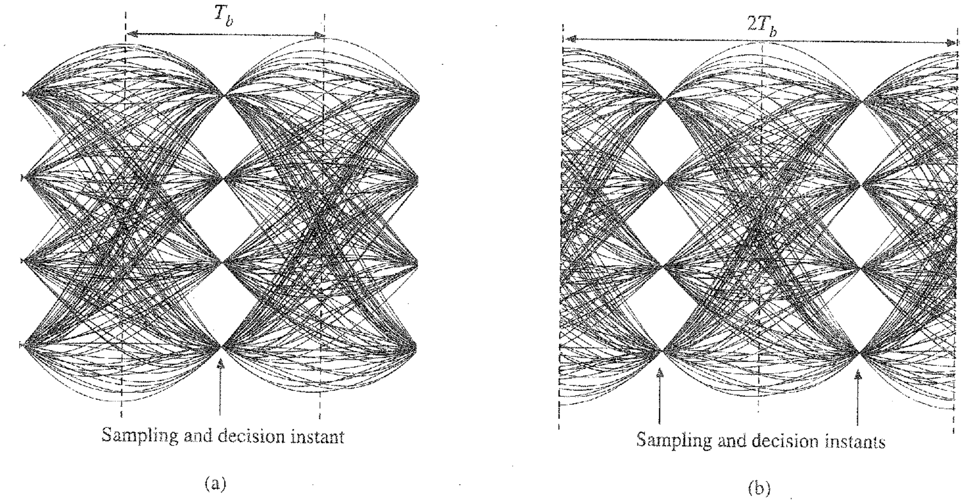

Figure 7.29 Eye diagrams of a 4-ary PAM signaling system using a raised-cosine pulse with roll-off factor 0.5: (a) over two symbol periods $2T_b$ with time offset $T_b/2$; (b) without time offset.

Eye diagrams can also be generated for M-ary PAM by using the same method used for binary modulations. Because of multilevel signaling, the eye diagram should have M levels at the optimum sampling instants even when ISI is zero. Here we generate the practical eye diagram example for a four-level PAM signal that uses the same cosine roll-off pulse with roll-off factor $r = 0.5$ that was used in the eye diagram of Fig. 7.27. The corresponding eye diagrams with time offsets of $T_b/2$ and 0 are given in Fig. 7.29a and b, respectively. Once again, no ISI is observed at the sampling instants. The eye diagrams clearly show four equally separated signal values without ISI at the optimum sampling points.

7.8 DIGITAL CARRIER SYSTEMS

Thus far, we have discussed baseband digital systems, where signals are transmitted directly without any shift in frequency. Because baseband signals have sizable power at low frequencies, they are suitable for transmission over a pair of wires and coaxial cables. Much of the modern communication is conducted this way. However, baseband signals cannot be transmitted over a radio link or satellites because this would necessitate impractically large antennas to efficiently radiate the low-frequency spectrum of the signal. Hence, for these applications, the signal spectrum must be shifted to a high-frequency range. A spectrum shift to higher frequencies is also required to transmit several messages simultaneously by sharing the large bandwidth of the transmission medium. As seen in Chapter 4, the spectrum of a signal can be shifted to a higher frequency by applying the baseband digital signal to modulate a high-frequency sinusoid (carrier).

In transmitting and receiving digital carrier signals, we need a modulator and demodulator to transmit and receive data. The two devices, **modulator** and **demodulator** are usually packaged in one unit called a **modem** for two-way (duplex) communications.

7.8.1 Basic Binary Carrier Modulations

There are two basic forms of carrier modulation: amplitude modulation and angle modulation. In amplitude modulation, the carrier amplitude is varied in proportion to the modulating signal (i.e., the baseband signal). This is shown in Fig. 7.30. An unmodulated carrier cos $\omega_c t$ is shown

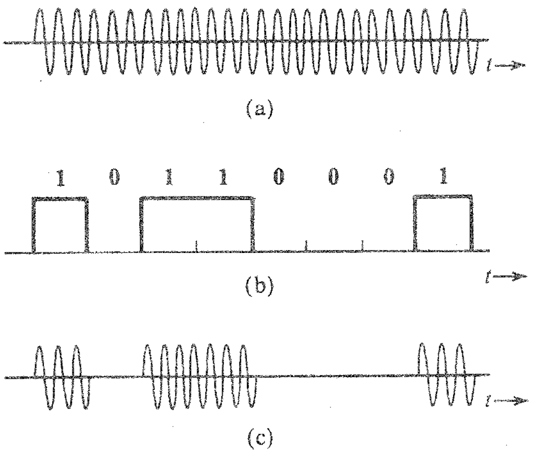

Figure 7.30 (a) The carrier $\cos \omega_c t$. (b) The modulating signal $m(t)$. (c) ASK: the modulated signal $m(t) \cos \omega_c t$.

in Fig. 7.30a. The on-off baseband signal $m(t)$ (the modulating signal) is shown in Fig. 7.30b. It can be written according to Eq. (7.1) as

$$m(t) = \sum a_k p(t - kT_b), \qquad \text{where} \qquad p(t) = \Pi\left(\frac{t - T_b/2}{T_b}\right)$$

The line code $a_k = 0,\ 1$ is on-off. When the carrier amplitude is varied in proportion to $m(t)$, we can write the carrier modulated signal as

$$\varphi_{\text{ASK}}(t) = m(t) \cos \omega_c t \tag{7.57}$$

shown in Fig. 7.30c. Note that the modulated signal is still an on-off signal. This modulation scheme of transmitting binary data is known as **on-off keying (OOK)** or **amplitude shift keying (ASK)**.

Of course, the baseband signal $m(t)$ may utilize a pulse $p(t)$ different from the rectangular one shown in the example of Fig. 7.30. This will generate an ASK signal that does not have a constant amplitude during the transmission of **1** ($a_k = 1$).

If the baseband signal $m(t)$ were polar (Fig. 7.31a), the corresponding modulated signal $m(t) \cos \omega_c t$ would appear as shown in Fig. 7.31b. In this case, if $p(t)$ is the basic pulse, we are transmitting **1** by a pulse $p(t) \cos \omega_c t$ and **0** by $-p(t) \cos \omega_c t = p(t) \cos (\omega_c t + \pi)$. Hence, the two pulses are π radians apart in phase. The information resides in the phase or the sign of the pulse. For this reason this scheme is known as **phase shift keying (PSK)**. Note that the transmission is still polar. In fact, just like ASK, the PSK modulated carrier signal has the same form

$$\varphi_{\text{PSK}}(t) = m(t) \cos \omega_c t \qquad m(t) = \sum a_k p(t - kT_b) \tag{7.58}$$

with the difference that the line code is polar $a_k = \pm 1$.

When data are transmitted by varying the frequency, we have the case of **frequency shift keying (FSK)**, as shown in Fig. 7.31c. A **0** is transmitted by a pulse of frequency ω_{c_0}, and **1** is transmitted by a pulse of frequency ω_{c_1}. The information about the transmitted data resides in the carrier frequency. The FSK signal may be viewed as a sum of two interleaved ASK signals, one with a modulating frequency ω_{c_0}, and the other with a modulating frequency ω_{c_1}. We can

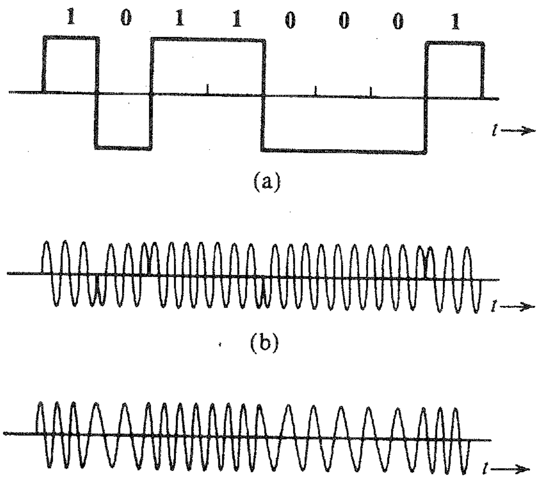

Figure 7.31 (a) The modulating signal $m(t)$. (b) PSK: the modulated signal $m(t) \cos \omega_c t$. (c) FSK: the modulated signal.

use the binary ASK expression of Eq. (7.57) to write the FSK signal as,

$$\varphi_{\text{FSK}}(t) = \sum a_k p(t - kT_b) \cos \omega_{c_1} t + \sum (1 - a_k) p(t - kT_b) \cos \omega_{c_0} t$$

where $a_k = 0, 1$ is on-off. Thus the FSK signal is a superposition of two AM signals with different carrier frequencies and different but complementary amplitudes.

In practice, ASK as an on-off scheme is commonly used today in optical fiber communications in the form of laser-intensity modulation. PSK is commonly applied in digital satellite communications and was also used in earlier telephone modems (2400 and 4800 bit/s). As for FSK, AT&T in 1962 developed one of the earliest telephone-line modems called 103A; it uses FSK to transmit 300 bit/s at two frequencies, 1070 and 1270 Hz, and receives FSK at 2025 and 2225 Hz.

7.8.2 PSD of Digital Carrier Modulation

We have just shown that the binary carrier modulations of ASK, PSK, and FSK can all be written into some forms of $m(t) \cos \omega_c t$. To determine the PSD of the ASK, PSK, and FSK signals, it would be helpful for us to first find the relationship between the PSD of $m(t)$ and the PSD of the modulated signal

$$\varphi(t) = m(t) \cos \omega_c t$$

Recall from Eq. (3.80) that the PSD of $\varphi(t)$ is

$$S_\varphi(f) = \lim_{T \to \infty} \frac{|\Psi_T(f)|^2}{T}$$

where $\Psi_T(f)$ is the Fourier transform of the truncated signal

$$\begin{aligned}\varphi_T(t) &= \varphi(t)[u(t+T/2) - u(t-T/2)] \\ &= m(t)[u(t+T/2) - u(t-T/2)]\cos\omega_c t \\ &= m_T(t)\cos\omega_c t \end{aligned} \tag{7.59}$$

Here $m_T(t)$ is the truncated baseband signal with Fourier transform $M_T(f)$. Applying the frequency shift property [see Eq. (3.36)], we have

$$\Psi_T(f) = \frac{1}{2}\left[M_T(f-f_c) + M_T(f+f_c)\right]$$

As a result, the PSD of the modulated carrier signal $\varphi(t)$ is

$$S_\varphi(f) = \lim_{T\to\infty} \frac{1}{4} \frac{|M_T(f+f_c) + M_T(f-f_c)|^2}{T}$$

Because $M(f)$ is a baseband signal, $M_T(f+f_c)$ and $M_T(f-f_c)$ have zero overlap as $T \to \infty$ as long as f_c is larger than the bandwidth of $M(f)$. Therefore, we conclude that

$$\begin{aligned}S_\varphi(f) &= \lim_{T\to\infty} \frac{1}{4}\left[\frac{|M_T(f+f_c)|^2}{T} + \frac{|M_T(f-f_c)|^2}{T}\right] \\ &= \frac{1}{4}S_M(f+f_c) + \frac{1}{4}S_M(f-f_c)\end{aligned} \tag{7.60}$$

In other words, for an appropriately chosen carrier frequency, modulation causes a shift in the baseband signal PSD.

Now, the ASK signal in Fig. 7.30c, fits this model, with $m(t)$ being an on-off signal (using a full-width or NRZ pulse). Hence, the PSD of the ASK signal is the same as that of an on-off signal (Fig. 7.4b) shifted to $\pm f_c$ as shown in Fig. 7.32a. Remember that by using a full-width rectangular pulse $p(t)$,

$$P\left(\frac{n}{T_b}\right) = 0 \qquad n = \pm 1, \pm 2, \ldots$$

In this case, the baseband on-off PSD has no discrete components except at dc in Fig. 7.30b. Therefore, the ASK spectrum has discrete component only at ω_c.

The PSK signal also fits this modulation description where $m(t)$ is a polar signal using a full-width NRZ pulse. Therefore, the PSD of a PSK signal is the same as that of the polar baseband signal shifted to $\pm\omega_c$, as shown in Fig. 7.32b. Note that this PSD has the same shape (with a different scaling factor) as the PSD of the ASK minus its discrete components.

Finally, we have shown that the FSK signal may be viewed as a sum of two interleaved ASK signals using the full-width pulse. Hence, the spectrum of FSK is the sum of two ASK spectra at frequencies ω_{c_0} and ω_{c_1}, as shown in Fig. 7.32c. It can be shown that by properly choosing ω_{c_0} and ω_{c_1} and by maintaining phase continuity during frequency switching, discrete components can be eliminated at ω_{c_0} and ω_{c_1}. Thus, no discrete components appear in this spectrum. It is important to note that the bandwidth of FSK is higher than that of ASK or PSK.

As observed earlier, polar signaling is the most power-efficient scheme. The PSK, being polar, requires 3 dB less power than ASK (or FSK) for the same noise immunity, that is, for the same error probability in pulse detection.

Figure 7.32 PSD of (a) ASK, (b) PSK, and (c) FSK.

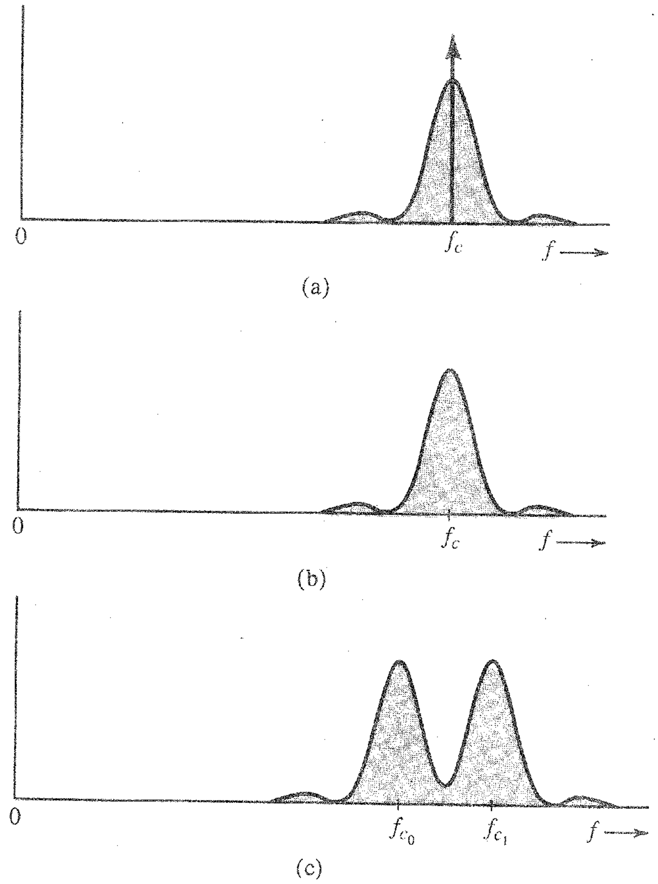

Of course, we can also modulate bipolar, or any other scheme discussed earlier. Also, note that the use of the NRZ rectangular pulse in Fig. 7.30 or 7.31 is for the sake of illustration only. In practice, baseband pulses may be spectrally shaped to eliminate ISI.

7.8.3 Connections between Analog and Digital Carrier Modulations

There is a natural and clear connection between ASK and AM because the message information is directly reflected in the varying amplitude of the modulated signals. Because of its nonnegative amplitude, ASK is essentially an AM signal with modulation index $\mu = 1$. There is a similar connection between FSK and FM. FSK is simply an FM signal with only limited number of instantaneous frequencies.

The connection between PSK and analog modulation is a bit more subtle. For PSK, the modulated signal can be written as

$$\varphi_{\text{PSK}}(t) = A\cos(\omega_c t + \theta_k) \qquad kT_b \le t < kT_b + T_b$$

It can therefore be connected with PM. However, a closer look at the PSK signal reveals that because of the constant phase θ_k, its instantaneous frequency, in fact, does not change. In fact, we can rewrite the PSK signal

$$\begin{aligned}\varphi_{\text{PSK}}(t) &= A\cos\theta_k \cos\omega_c t - A\sin\theta_k \sin\omega_c t \\ &= a_k \cos\omega_c t + b_k \sin\omega_c t \qquad kT_b \le t < kT_b + T_b \end{aligned} \tag{7.61}$$

by letting $a_k = A\cos\theta_k$ and $b_k = -A\sin\theta_k$. From Eq. (7.61), we recognize its strong resemblance to the QAM signal representation in Sec. 4.4. Therefore, the digital PSK modulation is closely connected with the analog QAM signal. In particular, $\theta = 0,\ \pi$ for binary PSK. Thus, binary PSK can be written as

$$\pm A\cos\omega_c t$$

This is effectively a digital manifestation of the DSB-SC amplitude modulation. In fact, as will be discussed later, by letting a_k take on multilevel values while setting $b_k = 0$ we can generate another digital carrier modulation known as the pulse amplitude modulation (or PAM), which can carry multiple bits during each modulation time-interval T_b.

As we have studied in Chapter 4, DSB-SC amplitude modulation is more power efficient than AM. Binary PSK is therefore more power efficient than ASK. In terms of bandwidth utilization, we can see from their connection to analog modulations that ASK and PSK have identical bandwidth occupation while FSK requires larger bandwidth. These observations intuitively corroborate our PSD results of Fig. 7.32.

7.8.4 Demodulation

Demodulation of digital-modulated signals is similar to that of analog-modulated signals. Because of the connections between ASK and AM, between FSK and FM, and between PSK and QAM (or DSB-SC AM), different demodulation techniques used for the analog modulations can be directly applied to their digital counterparts.

ASK Detection

Just like AM, ASK (Fig. 7.30c), can be demodulated both coherently (for synchronous detection) or noncoherently (for envelope detection). The coherent detector requires more elaborate equipment and has superior performance, especially when the signal power (hence SNR) is low. For higher SNR, the envelope detector performs almost as well as the coherent detector. Hence, coherent detection is not often used for ASK because it will defeat its very purpose (the simplicity of detection). If we can avail ourselves of a synchronous detector, we might as well use PSK, which has better power efficiency than ASK.

FSK Detection

Once again, the binary FSK can be viewed as two interleaved ASK signals with carrier frequencies ω_{c_0} and ω_{c_1}, respectively (Fig. 7.32c). Therefore, FSK can be detected coherently or noncoherently. In noncoherent detection, the incoming signal is applied to a pair of filters tuned to ω_{c_0} and ω_{c_1}, respectively. Each filter is followed by an envelope detector (see Fig. 7.33a). The outputs of the two envelope detectors are sampled and compared. If a **0** is transmitted by a pulse of frequency ω_{c_0}, then this pulse will appear at the output of the filter tuned to ω_{c_0}. Practically no signal appears at the output of the filter tuned to ω_{c_1}. Hence, the sample of the envelope detector output following the ω_{c_0} filter will be greater than the sample of the envelope

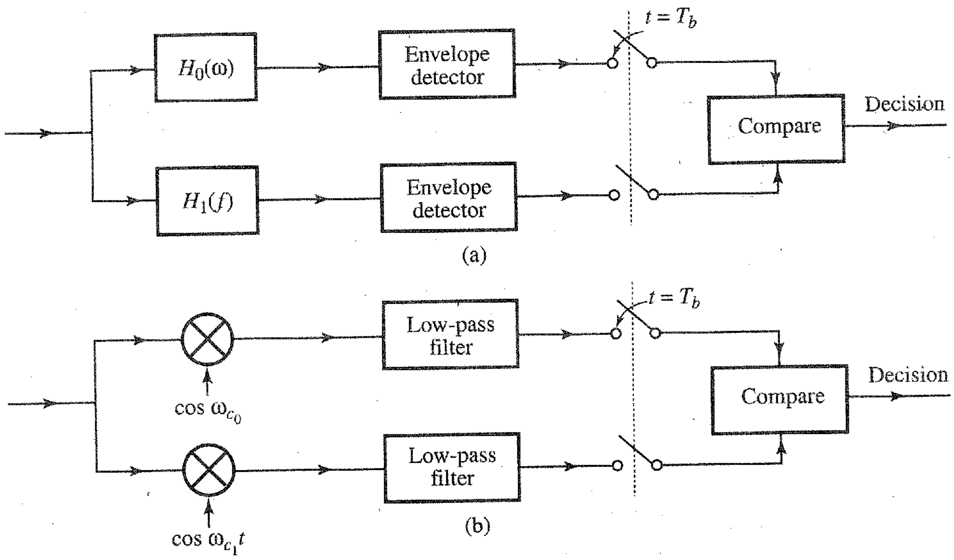

Figure 7.33 (a) Noncoherent detection of FSK. (b) Coherent detection of FSK.

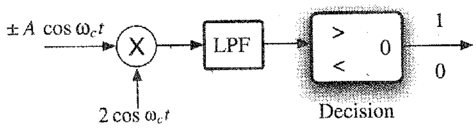

Figure 7.34 Coherent binary PSK detector (similar to a DSB-SC demodulator).

detector output following the ω_{c_1} filter, and the receiver decides that a **0** was transmitted. In the case of a **1**, the opposite happens.

Of course, FSK can also be detected coherently by generating two references of frequencies ω_{c_0} and ω_{c_1}, for the two demodulators, to demodulate the signal received and then comparing the outputs of the two demodulators as shown in Fig. 7.33b. Thus, coherent FSK detector must generate two carriers in synchronization with the modulation carriers. Once again, this complex demodulator defeats the purpose of FSK, which is designed primarily for simpler, noncoherent detection. In practice, coherent FSK detection is not in use.

PSK Detection

In binary PSK, a **1** is transmitted by a pulse $A \cos \omega_c t$ and a **0** is transmitted by a pulse $-A \cos \omega_c t$ (Fig. 7.31b). The information in PSK signals therefore resides in the carrier phase. Just as in DSB-SC, these signals cannot be demodulated via envelope detection because the envelope stays constant for both **1** and **0** (Fig. 7.31b). The coherent detector of the binary PSK modulation is shown in Fig. 7.34. The coherent detection is similar to that used for analog signals. Methods of carrier acquisition have been discussed in Sec. 4.8.

Differential PSK

Although envelope detection cannot be used for PSK detection, it is still possible to exploit the finite number of modulation phase values for noncoherent detection. Indeed, PSK signals may be demodulated noncoherently by means of an ingenious method known as **differential PSK**,

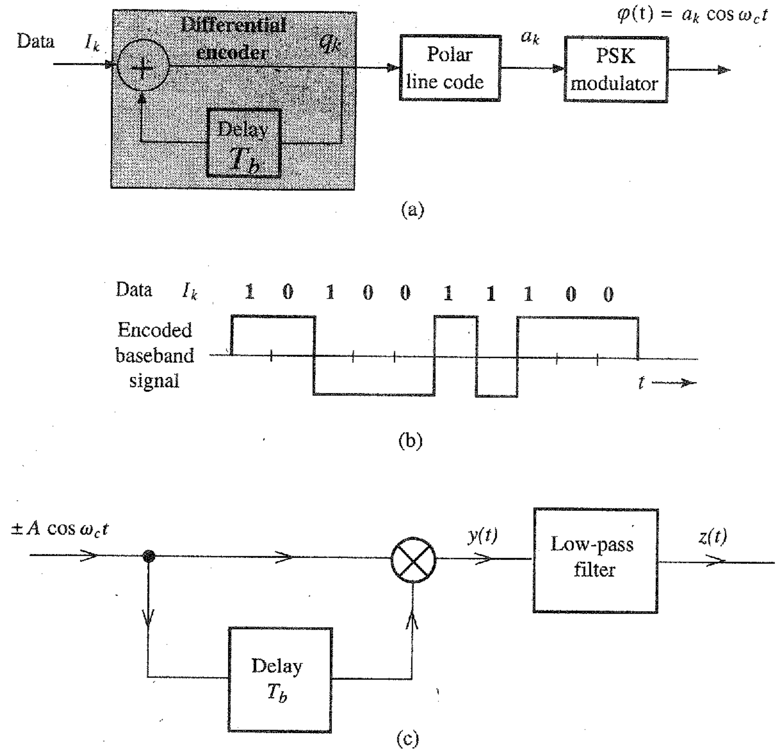

Figure 7.35 (a) Differential encoding; (b) encoded signal; (c) differential PSK receiver.

or DPSK. The principle of differential detection is for the receiver to detect the relative phase change between successive modulated phases θ_k and θ_{k-1}. Since the phase value in PSK is finite (equaling to 0 and π in binary PSK), the transmitter can encode the information data into the phase difference $\theta_k - \theta_{k-1}$. For example, a phase difference of zero represents **0** whereas a phase difference of π signifies **1**.

This technique is known as **differential encoding** (before modulation). In one differential code, a **0** is encoded by the same pulse used to encode the previous data bit (no transition), and a **1** is encoded by the negative of the pulse used to encode the previous data bit (transition). Differential encoding is simple to implement, as shown in Fig. 7.35a. Notice that the addition is modulo-2. The encoded signal is shown in Fig. 7.35b. Thus a transition in the line code pulse sequence indicates **1** and no transition indicates **0**. The modulated signal consists of pulses

$$A \cos(\omega_c t + \theta_k) = \pm A \cos \omega_c t$$

If the data bit is **0**, the present pulse and the previous pulse have the same polarity or phase; both pulses are either $A \cos \omega_c t$ or $-A \cos \omega_c t$. If the data bit is **1**, the present pulse and the previous pulse are of opposite polarities or phases; if the present pulse is $A \cos \omega_c t$, the previous pulse is $-A \cos \omega_c t$, and vice versa.

In demodulation of DPSK (Fig. 7.35c), we avoid generation of a local carrier by observing that the received modulated signal itself is a carrier ($\pm A \cos \omega_c t$) with a possible sign ambiguity. For demodulation, in place of the carrier, we use the received signal delayed by T_b (one bit interval). If the received pulse is identical to the previous pulse, the product $y(t) = A^2 \cos^2 \omega_c t = (A^2/2)(1 + \cos 2\omega_c t)$, and the low-pass filter output $z(t) = A^2/2$. We immediately detect the present bit as **0**. If the received pulse and the previous pulse are of

TABLE 7.3
Differential Encoding and Detection of Binary DPSK

Time k	0	1	2	3	4	5	6	7	8	9	10
I_k		1	0	1	0	0	1	1	1	0	0
q_k	0	1	1	0	0	0	1	0	1	1	1
Line code a_k	−1	1	1	−1	−1	−1	1	−1	1	1	1
θ_k	π	0	0	π	π	π	0	π	0	0	0
$\theta_k - \theta_{k-1}$		π	0	π	0	0	π	π	π	0	0
Detected bits		1	0	1	0	0	1	1	1	0	0

opposite polarity, $y(t) = -A^2 \cos^2 \omega_c t$ and $z(t) = -A^2/2$, and the present bit is detected as **0**. Table 7.3 illustrates a specific example of the encoding and decoding.

Thus, in terms of demodulation complexity, ASK, FSK, and DPSK can all be noncoherently detected without a synchronous carrier at the receiver. On the other hand, PSK must be coherently detected. Noncoherent detection, however, comes with a price in terms of noise immunity. From the point of view of noise immunity, coherent PSK is superior to all other schemes. PSK also requires smaller bandwidth than FSK (see Fig. 7.32). Quantitative discussion of this topic can be found in Chapter 10.

7.9 M-ARY DIGITAL CARRIER MODULATION

The binary digital carrier modulations of ASK, FSK, and PSK all transmit one bit of information over the interval of T_b second, or at the bit rate of $1/T_b$ bit/s. Similar to digital baseband transmission, higher bit rate transmission can be achieved either by reducing T_b or by applying M-ary signaling; the first option requires more bandwidth; the second requires more power. In most communication systems, bandwidth is strictly limited. Thus, to conserve bandwidth, an effective way to increase transmission data rate is to generalize binary modulation by employing M-ary signaling. Specifically, we can apply M-level ASK, M-frequency FSK, and M-phase PSK modulations.

M-ary ASK and Noncoherent Detection

M-ary ASK is a very simple generalization of binary ASK. Instead of sending only

$$\varphi(t) = 0 \text{ for } \mathbf{0} \qquad \text{and} \qquad \varphi(t) = A \cos \omega_c t \text{ for } \mathbf{1}$$

M-ary ASK can send $\log_2 M$ bits each time by transmitting, for example,

$$\varphi(t) = 0,\ A \cos \omega_c t,\ 2A \cos \omega_c t,\ \ldots,\ (M-1)A \cos \omega_c t$$

This is still an AM signal that uses M different amplitudes and a modulation index of $\mu = 1$. Its bandwidth remains the same as that of the binary ASK, while its power is increased proportionally with M^2. Its demodulation would again be achieved via envelope detection or coherent detection.

M-ary FSK and Orthogonal Signaling

M-FSK is similarly generated by selecting one sinusoid from the set $\{A \cos 2\pi f_i t,\ i = 1, \ldots, M\}$ to transmit a particular pattern of $\log_2 M$ bits. Generally for FSK, we can design a frequency increment δf and let

$$f_m = f_1 + (m-1)\delta f \qquad m = 1, 2, \ldots, M$$

For this FSK with equal frequency separation, the frequency deviation (in analyzing the FM signal) is

$$\Delta f = \frac{f_M - f_1}{2} = \frac{1}{2}(M-1)\delta f$$

It is therefore clear that the selection of the frequency set $\{f_i\}$ determines the performance and the bandwidth of the FSK modulation. If δf is chosen too large, then the M-ary FSK will use too much bandwidth. On the other hand, if δf is chosen too small, then over the time interval of T_b second, different FSK symbols will show virtually no difference and the receiver will be unable to distinguish the different symbols reliably. Thus large δf leads to bandwidth waste, whereas small δf is prone to detection error due to transmission noise and interference.

The task of M-ary FSK design is to determine a small enough δf that each FSK symbol $A \cos \omega_i t$ is highly distinct from all other FSK symbols. One solution to this problem of FSK signal design actually can be found in the discussion of orthogonal signal space in Sec. 2.6.2. If we can design FSK symbols to be orthogonal in T_b by selecting a small δf (or Δf), then the FSK signals will be truly distinct over T_b, and the bandwidth consumption will be small.

To find the minimum δf that leads to an orthogonal set of FSK signals, the orthogonality condition according to Sec. 2.6.2 requires that

$$\int_0^{T_b} A\cos(2\pi f_m t)\, A\cos(2\pi f_n t)\, dt = 0 \qquad m \neq n \tag{7.62}$$

We can use this requirement to find the minimum δf. First of all,

$$\begin{aligned}\int_0^{T_b} A\cos(2\pi f_m t)\, A\cos(2\pi f_n t)\, dt &= \frac{A^2}{2}\int_0^{T_b} [\cos 2\pi(f_m+f_n)t + \cos 2\pi(f_m-f_n)t]\, dt \\ &= \frac{A^2}{2}T_b \frac{\sin 2\pi(f_m+f_n)T_b}{2\pi(f_m+f_n)T_b} + \frac{A^2}{2}T_b \frac{\sin 2\pi(f_m-f_n)T_b}{2\pi(f_m-f_n)T_b}\end{aligned} \tag{7.63}$$

Since in practical modulations, $(f_m+f_n)T_b$ is very large (often no smaller than 10^3), the first term in Eq. (7.63) is effectively zero and negligible. Thus, the orthogonality condition reduces to the requirement that for any integer $m \neq n$,

$$\frac{A^2}{2}\frac{\sin 2\pi(f_m-f_n)T_b}{2\pi(f_m-f_n)} = 0$$

Because $f_m = f_1 + (m-1)\delta f$, for mutual orthogonality we have

$$\sin[2\pi(m-n)\delta f T_b] = 0 \qquad m \neq n$$

From this requirement, it is therefore clear that the smallest δf to satisfy the mutual orthogonality condition is

$$\delta f = \frac{1}{2T_b}\ \text{Hz}$$

This choice of minimum frequency separation is known as the *minimum shift* FSK. Since it forms an orthogonal set of symbols, it is often known as orthogonal signaling.

We can in fact describe the *minimum shift* FSK geometrically by applying the concept of orthonormal basis functions in Sec. 2.6. Let

$$\psi_i(t) = \sqrt{\frac{2}{T_b}} \cos 2\pi \left(f_1 + \frac{i-1}{2T_b}\right) t \qquad i = 1, 2, \ldots, M$$

It can be simply verified that

$$\int_0^{T_b} \psi_m(t)\psi_n(t)\, dt = \begin{cases} 1 & m = n \\ 0 & m \neq n \end{cases}$$

Thus, each of the FSK symbol can be written as

$$A \cos 2\pi f_m t = A\sqrt{\frac{T_b}{2}}\psi_m(t) \qquad m = 1, 2, \ldots, M$$

The geometrical relationship of the two FSK symbols for $M = 2$ is easily captured by Fig. 7.36.

The demodulation of M-ary FSK signals follows the same approach as the binary FSK demodulation. Generalizing the binary FSK demodulators of Fig. 7.33 we can apply a bank of M coherent or noncoherent detectors to the M-ary FSK signal before making a decision based on the strongest detector branch.

Earlier in the PSD analysis of baseband modulations, we showed that the baseband digital signal bandwidth at the symbol interval of T_b can be approximated by $1/T_b$. Therefore, for the minimum shift FSK, $\Delta f = (M-1)/(4T_b)$, and its bandwidth according to Carson's rule is approximately

$$2(\Delta f + B) = \frac{M-3}{2T_b}$$

In fact, it can be in general shown that the bandwidth of an orthogonal M-ary scheme is M times that of the binary scheme [see Sec. 10.7, Eq. (10.123)]. Therefore, in an M-ary orthogonal scheme, the rate of communication increases by a factor of $\log_2 M$ at the cost of M-fold transmission bandwidth increase. For a comparable noise immunity, the transmitted power is practically independent of M in the orthogonal scheme. Therefore, unlike M-ary ASK, M-ary FSK does not require more transmission power. However, its bandwidth requirement increases almost linearly with M (compared with binary FSK or M-ary ASK).

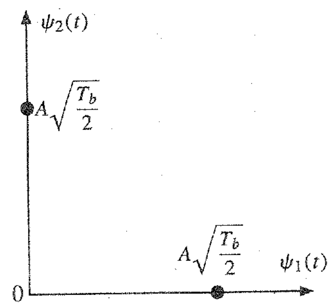

Figure 7.36 Binary FSK symbols in the two-dimensional orthogonal signal space.

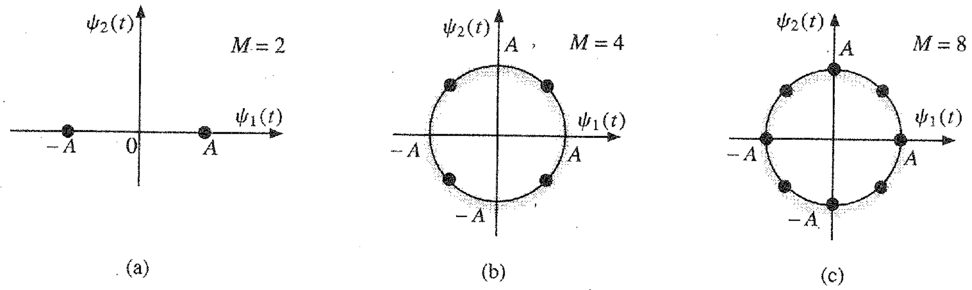

Figure 7.37 *M*-ary PSK symbols in the orthogonal signal space: (a) $M = 2$; (b) $M = 4$; (c) $M = 8$.

M-ary PSK, PAM, and QAM

By making a small modification to Eq. (7.61), PSK signals in general can be written into the format of

$$\varphi_{\text{PSK}}(t) = a_m\sqrt{\frac{2}{T_b}}\cos\omega_c t + b_m\sqrt{\frac{2}{T_b}}\sin\omega_c t \qquad 0 \le t < T_b \tag{7.64a}$$

in which $a_m = A\cos\theta_m$ and $b_m = -A\sin\theta_m$. In fact, based on the analysis in Sec. 2.6, $\sqrt{2/T_b}\cos\omega_c t$ and $\sqrt{2/T_b}\sin\omega_c t$ are orthogonal to each other. Furthermore, they are normalized over $[0, T_b]$. As a result, we can represent all PSK symbols in a two-dimensional signal space with basis functions

$$\psi_1(t) = \sqrt{\frac{2}{T_b}}\cos\omega_c t \qquad \psi_2(t) = \sqrt{\frac{2}{T_b}}\sin\omega_c t$$

such that

$$\varphi_{\text{PSK}}(t) = a_m\psi_1(t) + b_m\psi_2(t) \tag{7.64b}$$

We can geometrically illustrate the relationship of the PSK symbols in the signal space (Fig. 7.37). Equation (7.64) means that PSK modulations can be represented as QAM signal. In fact, because the signal is PSK, the signal points must meet a special requirement that

$$\begin{aligned} a_m^2 + b_m^2 &= A^2\cos^2\theta_m + (-A)^2\sin^2\theta_m \\ &= A^2 = \text{constant} \end{aligned} \tag{7.64c}$$

In other words, all the signal points must stay on a circle of radius A. In practice, all the signal points are chosen to be equally spaced in the interest of obtaining the best immunity against noise. Therefore, for M-ary PSK signaling, the angles are typically chosen uniformly as

$$\theta_m = \theta_0 + \frac{2\pi}{M}(m-1) \qquad m = 1, 2, \ldots, M$$

The special PSK signaling with $M = 4$ is an extremely popular and powerful digital modulation format.* It in fact is a summation of two binary PSK signals, one using the

* QPSK has several effective variations including the offset QPSK.

(in-phase) carrier of cos $\omega_c t$ while the other uses the (quadrature) carrier of sin $\omega_c t$ of the same frequency. For this reason, it is also known as **quadrature PSK (QPSK)**. We can transmit and receive both of these signals on the same channel, thus doubling the transmission rate.

To further generalize the PSK to achieve higher data rate, we can see that the PSK representation of Eq. (7.64) is a special case of the quadrature amplitude modulation (QAM) signal discussed in Chapter 4 (Fig. 4.19). The only difference lies in the requirement by PSK that the modulated signal have a constant magnitude (modulus) A. In fact, the much more flexible and general QAM signaling format can be conveniently used for digital modulation as well. The signal transmitted by an M-ary QAM system can be written as

$$\begin{aligned} p_i(t) &= a_i p(t) \cos \omega_c t + b_i p(t) \sin \omega_c t \\ &= r_i p(t) \cos (\omega_c t - \theta_i) \qquad i = 1, 2, \ldots, M \end{aligned}$$

where

$$r_i = \sqrt{a_i^2 + b_i^2} \qquad \text{and} \qquad \theta_i = \tan^{-1} \frac{b_i}{a_i} \tag{7.65}$$

and $p(t)$ is a properly shaped baseband pulse. The simplest choice of $p(t)$ would be a rectangular pulse

$$p(t) = \sqrt{\frac{2}{T_b}} \, [u(t) - u(t - T_b)]$$

Certainly, better pulses can also be applied conserve bandwidth.

Figure 7.38a shows the QAM modulator and demodulator. Each of the two signals $m_1(t)$ and $m_2(t)$ is a baseband $\sqrt{M}$-ary pulse sequence. The two signals are modulated by two carriers of the same frequency but in phase quadrature. The digital QAM signal $p_i(t)$ can be generated by means of QAM by letting $m_1(t) = a_i p(t)$ and $m_2(t) = b_i p(t)$. Both $m_1(t)$ and $m_2(t)$ are baseband PAM signals. The eye diagram of the QAM signal consists of the in-phase component $m_1(t)$ and the quadrature component $m_2(t)$. Both exhibit the M-ary baseband PAM eye diagram, as discussed earlier in Sec. 7.6.

The geometrical representation of M-ary QAM can be extended from the PSK signal space by simply removing the constant modulus constraint Eq. (7.64c). One very popular and practical choice of r_i and θ_i for $M = 16$ is shown graphically in Fig. 7.38b. The transmitted pulse $p_i(t)$ can take on 16 distinct forms, and is, therefore, a 16-ary pulse. Since $M = 16$, each pulse can transmit the information of $\log_2 16 = 4$ binary digits. This can be done as follows: there are 16 possible sequences of four binary digits and there are 16 combinations (a_i, b_i) in Fig. 7.38b. Thus, every possible four-bit sequence is transmitted by a particular (a_i, b_i) or (r_i, θ_i). Therefore, one signal pulse $r_i p(t) \cos (\omega_c t - \theta_i)$ transmits four bits. Compared with binary PSK (or BPSK), the 16-ary QAM bit rate is quadrupled without increasing the bandwidth. The transmission rate can be increased further by increasing the value of M.

Modulation as well as demodulation can be performed by using the system in Fig. 7.38a. The inputs are $m_1(t) = a_i p(t)$ and $m_2(t) = b_i p(t)$. The two outputs at the demodulator are $a_i p(t)$ and $b_i p(t)$. From knowledge of (a_i, b_i), we can determine the four transmitted bits. Further analysis of 16-ary QAM on a noisy channel is carried out in Sec. 10.6 [Eq. (10.104)]. The practical value of this 16-ary QAM signaling becomes fully evident when we consider its broad range of applications. In fact, 16-QAM is used in the V.32 telephone data/fax modems (9600 bit/s), in high-speed cable modems, and in modern satellite digital television broadcasting.

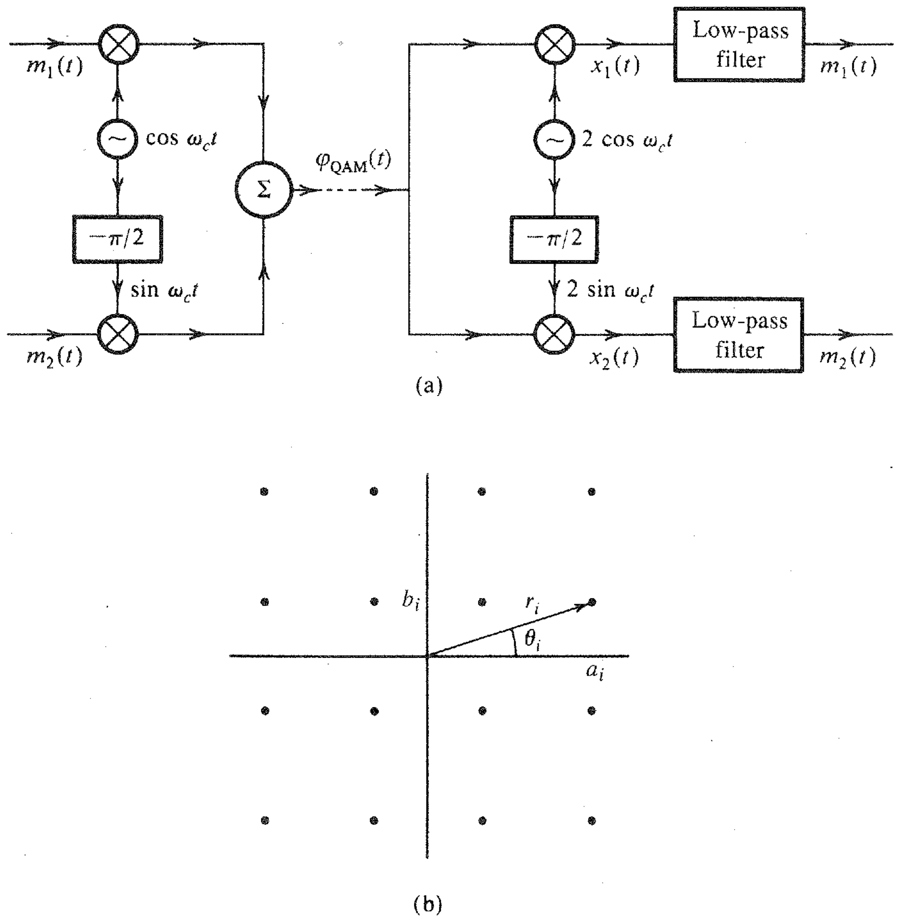

Figure 7.38 (a) QAM or quadrature multiplexing and (b) 16-point QAM ($M = 16$).

Note that if we disable the data stream that modulates sin $\omega_c t$ in QAM, then all the signaling points can be reduced to a single dimension. Upon setting $m_2(t) = 0$, QAM becomes

$$p_i(t) = a_i p(t) \cos \omega_c t, \qquad t \in [0, T_b]$$

This degenerates into the pulse amplitude modulation or PAM. Comparison of the signal expression of $p_i(t)$ with the analog DSB-SC signal makes it clear that PAM is the digital version of the DSB-SC signal. Just as analog QAM is formed by the superposition of two DSB-SC amplitude modulations in phase quadrature, digital QAM consists of two PAM signals, each having $\sqrt{M}$ signaling levels. Similarly, like the relationship between analog DSB-SC and QAM, PAM requires the same amount of bandwidth as QAM does. However, PAM is much less efficient because it would need M modulation signaling levels in one dimension, whereas QAM requires only $\sqrt{M}$ signaling levels in each of the two orthogonal QAM dimensions.

Trading Power and Bandwidth

In Chapter 10 we shall discuss several other types of M-ary signaling. The nature of the exchange between the transmission bandwidth and the transmitted power (or SNR) depends on the choice of M-ary scheme. For example, in orthogonal signaling, the transmitted power is practically independent of M but the transmission bandwidth increases with M. Contrast this to the PAM case, where the transmitted power increases roughly with M^2 while the bandwidth remains constant. Thus, M-ary signaling allows us great flexibility in trading signal power (or SNR) for transmission bandwidth. The choice of the appropriate system will depend upon the particular circumstances. For instance, it will be appropriate to use QAM signaling if the bandwidth is at a premium (as in telephone lines) and to use orthogonal signaling when power is at a premium (as in space communication).

7.10 MATLAB EXERCISES

In this section, we provide MATLAB programs to generate the eye diagrams. The first step is to specify the basic pulse shapes in PAM. The next four short programs are used to generate NRZ, RZ, half-sinusoid, and raised-cosine pulses.

```
% (pnrz.m)
% generating a rectangular pulse of width T
% Usage function pout=pnrz(T);
function pout=prect(T);
pout=ones(1,T);
end
```

```
% (prz.m)
% generating a rectangular pulse of width T/2
% Usage function pout=prz(T);
function pout=prz(T);
pout=[zeros(1,T/4) ones(1,T/2) zeros(1,T/4)];
end
```

```
% (psine.m)
% generating a sinusoid pulse of width T
%
function pout=psine(T);
pout=sin(pi*[0:T-1]/T);
end
```

```
% (prcos.m)
%  Usage   y=prcos(rollfac,length, T)
function y=prcos(rollfac,length, T)
% rollfac = 0 to 1 is the rolloff factor
% length is the onesided pulse length in the number of T
% length = 2T+1;
% T is the oversampling rate
y=rcosfir(rollfac, length, T,1, 'normal');
end
```

The first program (binary_eye.m) uses the four different pulses to generate eye diagrams of binary polar signaling.

```
% (binary_eye.m)
% generate and plot eyediagrams
%
clear;clf;
data = sign(randn(1,400));  % Generate 400 random bits
Tau=64;                     % Define the symbol period
dataup=upsample(data, Tau); % Generate impulse train
yrz=conv(dataup,prz(Tau));  % Return to zero polar signal
yrz=yrz(1:end-Tau+1);
ynrz=conv(dataup,pnrz(Tau)); % Non-return to zero polar
ynrz=ynrz(1:end-Tau+1);
ysine=conv(dataup,psine(Tau));  % half sinusoid polar
ysine=ysine(1:end-Tau+1);
Td=4;                       % truncating raised cosine to 4 periods
yrcos=conv(dataup,prcos(0.5,Td,Tau)); % rolloff factor = 0.5
yrcos=yrcos(2*Td*Tau:end-2*Td*Tau+1); % generating RC pulse train
eye1=eyediagram(yrz,2*Tau,Tau,Tau/2);title('RZ eye-diagram');
eye2=eyediagram(ynrz,2*Tau,Tau,Tau/2);title('NRZ eye-diagram');
eye3=eyediagram(ysine,2*Tau,Tau,Tau/2);title('Half-sine eye-diagram');
eye4=eyediagram(yrcos,2*Tau,Tau); title('Raised-cosine eye-diagram');
```

The second program (Mary_eye.m) uses the four different pulses to generate eye diagrams of four-level PAM signaling.

```
% (Mary_eye.m)
% generate and plot eyediagrams
%
%
clear;clf;
data = sign(randn(1,400))+2* sign(randn(1,400)); % 400 PAM symbols
Tau=64;                     % Define the symbol period
dataup=upsample(data, Tau); % Generate impulse train
yrz=conv(dataup,prz(Tau));  % Return to zero polar signal
yrz=yrz(1:end-Tau+1);
ynrz=conv(dataup,pnrz(Tau)); % Non-return to zero polar
ynrz=ynrz(1:end-Tau+1);
ysine=conv(dataup,psine(Tau));  % half sinusoid polar
ysine=ysine(1:end-Tau+1);
Td=4;                       % truncating raised cosine to 4 periods
yrcos=conv(dataup,prcos(0.5,Td,Tau)); % rolloff factor = 0.5
yrcos=yrcos(2*Td*Tau:end-2*Td*Tau+1); % generating RC pulse train
eye1=eyediagram(yrz,2*Tau,Tau,Tau/2);title('RZ eye-diagram');
eye2=eyediagram(ynrz,2*Tau,Tau,Tau/2);title('NRZ eye-diagram');
eye3=eyediagram(ysine,2*Tau,Tau,Tau/2);title('Half-sine eye-diagram');
eye4=eyediagram(yrcos,2*Tau,Tau); title('Raised-cosine eye-diagram');
```

REFERENCES

1. A. Lender, "Duobinary Technique for High Speed Data Transmission," *IEEE Trans. Commun. Electron.*, vol. CE-82, pp. 214–218, May 1963.
2. A. Lender, "Correlative Level Coding for Binary-Data Transmission," *IEEE Spectrum*, vol. 3, no. 2, pp. 104–115, Feb. 1966.
3. P. Bylanski and D. G. W. Ingram, *Digital Transmission Systems*, Peter Peregrinus Ltd., Hertshire, England, 1976.
4. H. Nyquist, "Certain Topics in Telegraph Transmission Theory," *AIEE Trans.*, vol. 47, p. 817, April 1928.
5. E. D. Sunde, *Communication Systems Engineering Technology*, Wiley, New York, 1969.
6. R. W. Lucky and H. R. Rudin, "Generalized Automatic Equalization for Communication Channels," *IEEE Int. Commun. Conf.*, vol. 22, 1966.
7. W. F. Trench, "An Algorithm for the Inversion of Finite Toeplitz Matrices," *J. SIAM*, vol. 12, pp. 515–522, Sept. 1964.
8. A. Lender, Chapter 7, in *Digital Communications: Microwave Applications*, K. Feher, Ed., Prentice-Hall, Englewood Cliffs, NJ, 1981.

PROBLEMS

7.2-1 Consider a full-width rectangular pulse shape

$$p(t) = \Pi(t/T_b)$$

(a) Find PSDs for the polar, on-off, and bipolar signaling.

(b) Sketch roughly the PSDs and find their bandwidths. For each case, compare the bandwidth to the case where $p(t)$ is a half-width rectangular pulse.

7.2-2 **(a)** A random binary data sequence **110100101**$\cdots$ is transmitted by using a Manchester (split-phase) line code with the pulse $p(t)$ shown in Fig. 7.7a. Sketch the waveform $y(t)$.

(b) Derive $S_y(f)$, the PSD of a Manchester (split-phase) signal in part **(a)** assuming **1** and **0** equally likely. Roughly sketch this PSD and find its bandwidth.

7.2-3 If the pulse shape is

$$p(t) = \Pi\left(\frac{t}{0.5T_b}\right)$$

use differential code (see Fig. 7.18) to derive the PSD for a binary signal. Determine the PSD $S_y(f)$.

7.2-4 The **duobinary** line coding proposed by Lender is also ternary like bipolar, but it requires only half the bandwidth of bipolar. In practice, duobinary coding is indirectly realized by using a special pulse shape as discussed in Sec. 7.3 (see Fig. 7.18). In this code, a **0** is transmitted by no pulse, and a **1** is transmitted by a pulse $p(t)$ or $-p(t)$ using the following rule. A **1** is encoded by the same pulse as that used for the previous **1** if there are an even number of **0**s between them. It is encoded by a pulse of opposite polarity if there are an odd number of **0**s between them. A number 0 is considered to be an even number. Like bipolar, this code also has a single error detection capability, because correct reception implies that between successive pulses of the same polarity, an even number of **0**s must occur, and between successive pulses of opposite polarity, an odd number of **0**s must occur.

(a) Assuming half-width rectangular pulse, sketch the duobinary signal $y(t)$ for the random binary sequence

1110001101001010 ···

(b) Determine R_0, R_1, and R_2 for this code. Assume (or you may show if you like) that $R_n = 0$ for all $n > 2$. Find and sketch the PSD for this line code (assuming half-width pulse). Show that its bandwidth is $R_b/2$ Hz, half that of bipolar.

7.3-1 Data at a rate of 6 kbit/s is to be transmitted over a leased line of bandwidth 4 kHz by using Nyquist criterion pulses. Determine the maximum value of the roll-off factor r that can be used.

7.3-2 In a certain telemetry system, there are eight analog measurements, each of bandwidth 2 kHz. Samples of these signals are time-division-multiplexed, quantized, and binary-coded. The error in sample amplitudes cannot be greater than 1% of the peak amplitude.

(a) Determine L, the number of quantization levels.

(b) Find the transmission bandwidth B_T if Nyquist criterion pulses with roll-off factor $r = 0.2$ are used. The sampling rate must be at least 25% above the Nyquist rate.

7.3-3 A leased telephone line of bandwidth 3 kHz is used to transmit binary data. Calculate the data rate (in bits per second) that can be transmitted if we use:

(a) Polar signal with rectangular half-width pulses.

(b) Polar signal with rectangular full-width pulses.

(c) Polar signal using Nyquist criterion pulses of $r = 0.25$.

(d) Bipolar signal with rectangular half-width pulses.

(e) Bipolar signal with rectangular full-width pulses.

7.3-4 The Fourier transform $P(f)$ of the basic pulse $p(t)$ used in a certain binary communication system is shown in Fig. P7.3-4.

(a) From the shape of $P(f)$, explain at what pulse rate this pulse would satisfy Nyquist's criterion.

(b) Find $p(t)$ and verify that this pulse does (or does not) satisfy the Nyquist's criterion.

(c) If the pulse does satisfy the Nyquist criterion, what is the transmission rate (in bits per second) and what is the roll-off factor?

Figure P.7.3-4

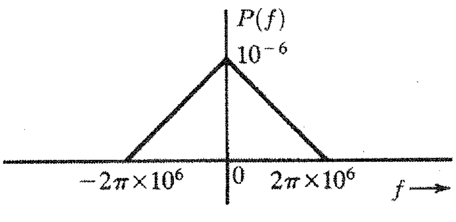

7.3-5 A pulse $p(t)$ whose spectrum $P(f)$ is shown in Fig. P7.3-5 satisfies Nyquist's criterion. If $f_1 = 0.8$ MHz and $f_2 = 1.2$ MHz, determine the maximum rate at which binary data can be transmitted by this pulse using Nyquist's criterion. What is the roll-off factor?

7.3-6 Binary data at a rate of 1 Mbit/s is to be transmitted by using Nyquist criterion pulses with $P(f)$ shown in Fig. P7.3-5, The frequencies f_1 and f_2 of the spectrum are adjustable. The channel available for the transmission of this data has a bandwidth of 700 kHz. Determine f_1 and f_2 and the roll-off factor.

Figure P.7.3-5

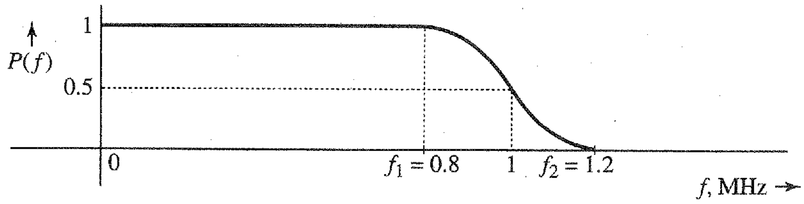

7.3-7 Show that the inverse Fourier transform of $P(f)$ in Eq. (7.39) is indeed second criterion pulse $p(t)$ given in Eq. (7.38).

Hint: Use Eq. (3.32) to find the inverse transform of $P(f)$ in Eq. (7.39) and express sinc (x) in the form $\sin x/x$.

7.3-8 Show that the inverse Fourier transform of $P(f)$ (the raised cosine pulse spectrum in Eq. (7.35) is the pulse $p(t)$ given in Eq (7.36).

Hint: Use Eq. (3.32) to find the inverse transform of $P(f)$ in Eq. (7.39) and express sinc (x) in the form $\sin x/x$.

7.3-9 Show that there exists one (and only one) pulse $p(t)$ of bandwidth $R_b/2$ Hz that satisfies the criterion of second criterion pulse [Eq. (7.37)]. Show that this pulse is given by

$$p(t) = \{\text{sinc}\,(\pi R_b t) + \text{sinc}\,[\pi R_b(t - T_b)]\} = \frac{\sin\,(\pi R_b t)}{\pi R_b t(1 - R_b t)}$$

and its Fourier transform is $P(f)$ given in Eq. (7.39).

Hint: For a pulse of bandwidth $R_b/2$, the Nyquist interval is $1/R_b = T_b$, and the conditions (7.37) give the Nyquist sample values at $t = \pm nT_b$. Use the interpolation formula [Eq. (6.10)] with $B = R_b/2$, $T_s = T_b$ to construct $p(t)$. In determining $P(f)$, recognize that $(1+e^{-j2\pi f T_b}) = e^{-j\pi f T_b}(e^{j\pi f T_b} + e^{-j\pi f T_b 2})$.

7.3-10 In a binary data transmission using duobinary pulses, sample values were read as follows:

$$1\,2\,0\ -2\ -2\,0\,0\ -2\,0\,2\,0\,0\,2\,0\,0\,0\ -2$$

(a) Explain if there is any error in detection.

(b) If there is no detection error, determine the received bit sequence.

7.3-11 In a binary data transmission using duobinary pulses, sample values of the received pulses were read as follows:

$$1\,2\,0\,0\,0\ -2\,0\,0\ -2\,0\,2\,0\,0\ -2\,0\,2\,2\,0\ -2$$

(a) Explain if there is any error.

(b) Can you guess the correct transmitted digit sequence? There is more than one possible correct sequence. Give as many correct sequences as possible, assuming that more than one detection error is extremely unlikely.

7.4-1 In Example 7.2, when the sequence S = **101010100000111** was applied to the input of the scrambler in Fig. 7.20a, the output T was found to be **101110001101001**. Verify that when this sequence T is applied to the input of the descrambler in Fig. 7.20b, the output is the original input sequence, $S =$ **101010100000111**.

7.4-2 Design a descrambler for the scrambler of Fig. P7.4-2. If a sequence $S =$ **101010100000111**. is applied to the input of this scrambler, determine the output sequence T. Verify that if this T is applied to the input of the descrambler, the output is the sequence S.

Figure P.7.4-2

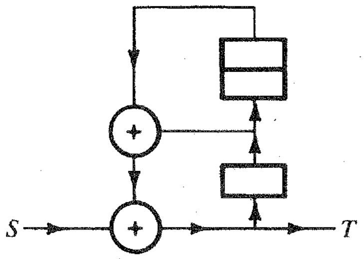

7.4-3 Repeat Prob. 7.4-2 if the scrambler shown in Fig. P7.4-3 is concatenated with the scrambler in Fig. P7.4-2 to form a composite scrambler.

Figure P.7.4-3

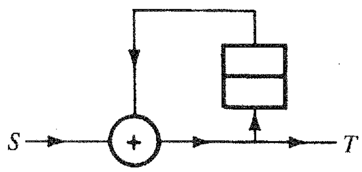

7.5-1 In a certain binary communication system that uses Nyquist's criterion pulses, a received pulse $p_r(t)$ (see Fig. 7.22a) has the following nonzero sample values:

$$p_r(0) = 1$$
$$p_r(T_b) = 0.1 \qquad p_r(-T_b) = 0.3$$
$$p_r(2T_b) = -0.02 \qquad p_r(-2T_b) = -0.07$$

(a) Determine the tap settings of a three-tap, zero-forcing equalizer.

(b) Using the equalizer in part **(a)**, find the residual nonzero ISI.

7.7-1 In a PAM scheme with $M = 16$:

(a) Determine the minimum transmission bandwidth required to transmit data at a rate of 12,000 bits/sec with zero ISI.

(b) Determine the transmission bandwidth if Nyquist criterion pulses with a roll-off factor $r = 0.2$ are used to transmit data.

7.7-2 An audio signal of bandwidth 4 kHz is sampled at a rate 25% above the Nyquist rate and quantized. The quantization error is not to exceed 0.1% of the signal peak amplitude. The resulting quantized samples are now coded and transmitted by 4-ary pulses.

(a) Determine the minimum number of 4-ary pulses required to encode each sample.

(b) Determine the minimum transmission bandwidth required to transmit this data with zero ISI.

(c) If 4-ary pulses satisfying Nyquist's criterion with 25% roll-off are used to transmit this data, determine the transmission bandwidth.

7.7-3 Binary data is transmitted over a certain channel at a rate R_b bit/s. To reduce the transmission bandwidth, it is decided to use 16-ary PAM signaling to transmit this data.

(a) By what factor is the bandwidth reduced?

(b) By what factor is the transmitted power increased, assuming minimum separation between pulse amplitudes to be the same in both cases?

Hint: Take the pulse amplitudes to be $\pm A/2$, $\pm 3A/2$, $\pm 5A/2$, $\pm 7A/2, \cdots, \pm 15A/2$ so that the minimum separation between various amplitude levels is A (same as that in the binary case pulses $\pm A/2$). Assume that all 16 levels are equally likely. Recall also that multiplying a pulse by a constant k increases its energy k^2-fold.

7.7-4 An audio signal of bandwidth 10 kHz is sampled at a rate of 24 kHz, quantized into 256 levels and coded by means of M-ary PAM pulses satisfying Nyquist's criterion with a roll-off factor $r = 0.2$. A 30 kHz bandwidth is available to transmit the data. Determine the best value of M.

7.7-5 Consider a case of binary transmission via polar signaling that uses half-width rectangular pulses of amplitudes $A/2$ and $-A/2$. The data rate is R_b bit/s.

(a) What is the minimum transmission bandwidth and the transmitted power.

(b) This data is to be transmitted by M-ary rectangular half-width pulses of amplitudes

$$\pm A/2,\ \pm 3A/2,\ \pm 5A/2, \ldots, \pm[(M-1)/2]A$$

Note that to maintain about the same noise immunity, the minimum pulse amplitude separation is A. If each of the M-ary pulses is equally likely to occur, show that the transmitted power is

$$P = \frac{(M^2-1)A^2}{24 \log_2 M}$$

Also determine the transmission bandwidth.

7.8-1 Figure P7.8-1 shows a binary data transmission scheme. The baseband signal generator uses full-width pulses and polar signaling. The data rate is 1 Mbit/s.

(a) If the modulator generates a PSK signal, what is the bandwidth of the modulated output?

(b) If the modulator generates FSK with the difference $f_{c1} - f_{c0} = 100$ kHz (see Fig. 7.32c), determine the modulated signal bandwidth.

Figure P.7.8-1

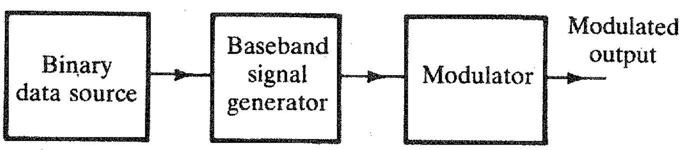

7.8-2 Repeat Prob. 7.8-1 if, instead of full-width pulses, Nyquist's criterion pulses with $r = 0.2$ are used.

7.8-3 Repeat Prob. 7.8-1 if a multiamplitude scheme with $M = 4$ (PAM signaling with full-width pulse) is used. In FSK [Prob. 7.8-1, part (b)], assume that successive amplitude levels are transmitted by frequencies separated by 100 kHz.